Digest Journal of Nanomaterials and Biostructures Vol. 10, No. 1, January - March 2015, p. 221 - 229

ON THE STRUCTURAL, MORPHOLOGICAL AND OPTICAL PROPERTIES OF ITO, ZnO, ZnO:Al AND NiO THIN FILMS OBTAINED BY THERMAL OXIDATION

S. IFTIMIE[a,b], R. MALLET[c], J. MERIGEON[a], L. ION[b], M. GIRTAN[a], S. ANTOHE[b,d,*]

[a]*LPHIA Laboratory, LUNAM-Angers University, 2 Boulevard Lavoisier, 49045 Angers cedex 01, France*

[b]*MDEO Research & Development Center, Faculty of Physics, University of Bucharest, Atomistilor 405, Magurele-Ilfov, 077125, Romania*

[c]*SCIAM, LUNAM-Angers University, 4 Rue Larrey, 49933 Angers cedex 09, France*

[d]*Academy of Romanian Scientists, 54 Splaiul Independenţei, Bucharest*

Tin doped indium oxide, zinc oxide, aluminum doped zinc oxide and nickel oxides were obtained by thermal oxidation of metallic films deposited by magnetron sputtering in two substrate configurations: perpendicular and parallel to the plasma flow. The morphological, structural and optical properties of metallic and oxidized films were studied and compared. The optical characterization of oxide films revealed a very good transmittance in visible range. The morphological and structural analyses show a crystalline and compact structure for the obtained thin films. The influence of the deposition configuration on films' roughness is clear no matter of the nature of the deposited films.

(Received January 30, 2015; Accepted March 11, 2015)

Keywords: Oxide materials, Thin films, X-ray diffraction, AFM

1. Introduction

ITO, ZnO, AZO, SnO_2:F and NiO are frequently used as transparent layers for electrodes, optical spacers, electrochromic or buffer layers for solar cells based thin films. The surface morphology of these films may influence the devices functioning either by an increase of the active area or by conducting to short-circuits. Generally, oxide films are obtained by various chemical or physical methods such as spray pyrolysis [1-5], sputtering [6,7] or reactive sputtering [8,9], sol gel [10-12], ultrasonic chemical vapor deposition [13], pulsed laser deposition [14-15], etc. In this paper we present a different method to obtain transparent oxide thin films: thermal oxidation of metallic thin films. This method involves the deposition of metallic films followed by their thermal oxidation in open atmosphere. If there are some studies on In_2O_3 [16,17] and ZnO [18-25] thin films obtained by oxidation, at this moment we didn't find any report on ITO, AZO, or NiO films obtained by direct oxidation. The aim of this work was to investigate the growth and the structural, morphological and optical properties of transparent oxide films obtained by oxidation of metallic layers deposited by sputtering in two target-substrate configurations: parallel and perpendicular to the plasma flow. We denote "horizontal" the configuration in which the substrate was placed horizontally in the deposition chamber; that means for our arrangement parallel to the target and perpendicular to the plasma flow. The "vertical" configuration corresponds to parallel direction to the plasma flow of the substrate and perpendicular to the target

[*]Corresponding author: santohe@solid.fizica.unibuc.ro

direction. From our previous studies concerning the deposition of zinc metallic films by thermal vacuum evaporation we observed that the films' growth structure depends on the geometry of the deposition system [18,19]. Comparing to reactive sputtering or sputtering from ceramics targets, the advantages of this method are related with less energy consuming and an easier control of the work parameters.

2. Materials and methods

Metallic tin doped indium (In:Sn), zinc (Zn), zinc doped aluminum (Zn:Al) and nickel (Ni) thin films were deposited in two configurations, vertical and horizontal, onto optical glass substrates by magnetron sputtering, followed by direct thermal oxidation, in open atmosphere. The glass substrates were cleaned in ultrasonic bath using acetone and isopropyl for 15 minutes each procedure. All samples were deposited under argon atmosphere at 9×10^{-3} mbar. The deposition time was the same for all the samples, 2 minutes. The sputter current was adapted taking into account the target nature in order to obtain thin films with comparable thicknesses. The purity of all used material targets was higher than 99,9 %. The composition of In:Sn target was: 90% wt. In : 10% wt. Sn, and for Zn:Al target: 98% wt. Al and 2% wt. Zn. The oxidation process was performed by gradually heating from room temperature (RT) to 550°C, and the samples were maintained at this temperature until they became completely transparent. The thicknesses of the metallic and oxide films were determined using a Dektak 6M profilometer from Veeco™, and the obtained values were around 40 nm for those deposited in vertical configuration and around 150 nm for those in horizontal configuration.

The samples' morphology was investigated by atomic force microscopy (AFM), in contact mode, and by scanning electron microscopy (SEM). The structural characteristics were determined using a Brucker D8 diffractometer, CuKα radiation.

The optical investigations were made using a Perkin Elmer Lambda 35 spectrometer, at room temperature.

3. Results and Discussion

3.1. Structural investigations

Fig. 1 present the diffraction patterns for oxidized films obtained from metallic layers deposited in both configurations, vertical and horizontal. The identification of the peaks position was done by using the ASTM data files, as follow: ITO, pdf2 71-2194 (In_2O_3), pdf2 89-4596 ($In_{1.94}Sn_{0.0603}$); ZnO, pdf2 36-1451; ZnO:Al, pdf2 36-1451; NiO, pdf2 44-1159 (rhombohedral), pdf2 47-1049 and pdf2 71-1179 (face centered cubic).

No matter the film nature or deposition configuration, all samples showed a well-defined crystalline structure without a pronounced preferentially growth direction indicating the presence of the appropriate compounds with randomly oriented microcrystallites. The higher intensity of peaks for films deposited in horizontal arrangement is due to the higher thickness of these films.

It is well known that the thermal oxidation rate of the metallic films depends on the oxidation time, film thickness, oxidation temperature and, also, on the crystallographic orientation [26]. Heating the metallic films up to 550°C leads to a complete oxidation and no metal traces were observed from XRD analysis.

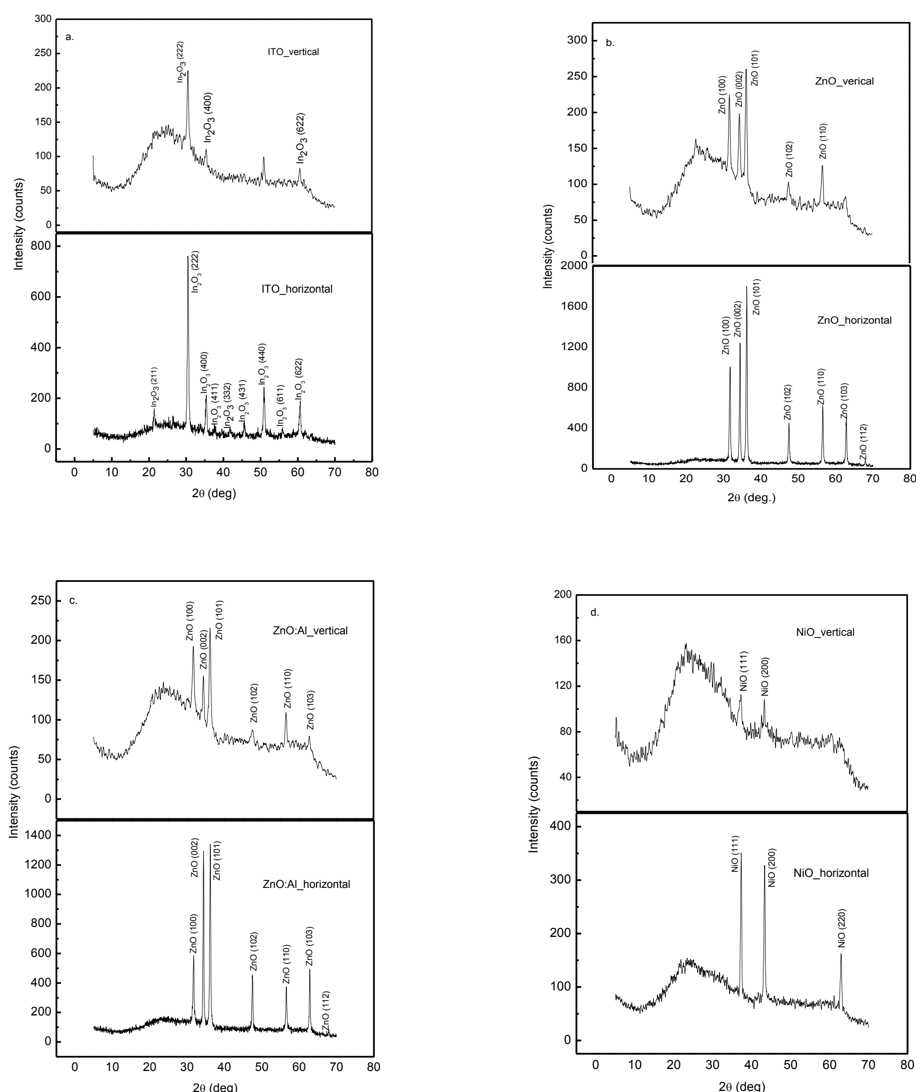

Fig. 1. XRD patterns for ITO, ZnO, AZO and NiO thin films obtained by direct oxidation

The grain sizes, determined using Scherrer's formula, are given in Table 1. The obtained values for oxide thin films, except NiO, depend slightly on the initial configurations of the metallic films. Concerning ZnO films tendency for a preferential crystalline direction corresponding to (101) was observed, unlike to the films obtained by oxidation of metallic layers deposited by thermal vacuum evaporation for which the preferential crystalline growth correspond to (002) plane [18].

Table1. Average grain size from XRD analysis for the prepared oxide thin films

	Deposition configuration	
Material	Horizontal (nm)	Vertical (nm)
ITO	25.2	24.3
ZnO	20.5	21.0
AZO	26.1	20.9
NiO	40.0	21.4

3.2. Morphological characterization

The morphology of the metallic thin films and the obtained oxides were investigated by atomic force microscopy (AFM, contact mode) and scanning electron microscopy (SEM), for both deposition arrangements – horizontal and vertical.

Table2. AFM calculated parameters for the prepared metallic and oxide thin films in horizontal configuration

Metal			Oxide		
Material	R_{RMS} (nm)	R_a (nm)	**Material**	R_{RMS} (nm)	R_a (nm)
In:Sn	125.0	108.0	**ITO**	117.0	87.0
Zn	61.3	45.8	**ZnO**	120.0	116.0
Zn:Al	30.8	24.1	**ZnO:Al**	90.0	60.0
Ni	16.0	14.0	**NiO**	18.0	14.0

Table3. AFM calculated parameters for the prepared metallic and oxide thin films in vertical configuration

Metal			Oxide		
Material	R_{RMS} (nm)	R_a (nm)	**Material**	R_{RMS} (nm)	R_a (nm)
In:Sn	3.4	2.2	**ITO**	11.0	5.7
Zn	21.0	15.0	**ZnO**	27.2	28.4
Zn:Al	10.8	7.3	**ZnO:Al**	26.0	27.0
Ni	17.0	14.0	**NiO**	11.0	8.4

The specific parameters, like root-mean-square roughness (R_{RMS}) defined as standard deviation of the Z-values for the investigated sample area and roughness average (R_a) defined as mean value of the surface height relative to the center of the investigated area, were calculated for both, metallic and oxide thin films. Table 2 gives the values obtained for samples prepared in horizontal configuration and Table 3 for the vertical ones.

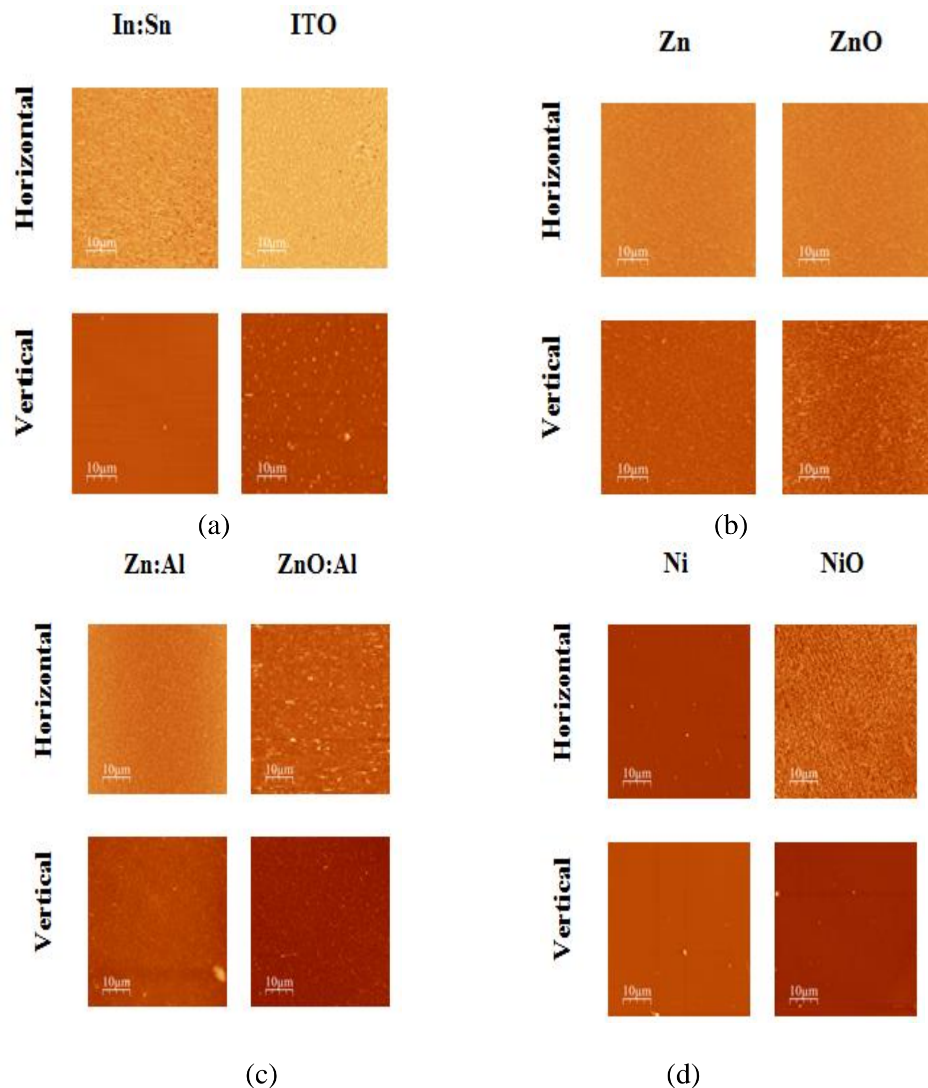

Fig.2. AFM images for metallic and oxide thin films obtained in both arrangements, vertical and horizontal

We observed that the roughness of the metallic thin films, as the roughness of the respective oxide films was higher for the films deposited in horizontal arrangement than for those vertically obtained. Since the crystallites sizes are similar for both horizontal and vertical arrangements we may assume that the difference in roughness is due to a different crystallites packing. In sputtering and evaporation deposition the crystal growth depend on the deposition rate but also on the chamber deposition geometry. For our prepared samples the deposition rate was around 72-75 nm/min for those deposited in horizontal arrangement (value obtained usually in the case of undoped and doped ZnO thin films prepared by sputtering [27-30]) and around 17-21 nm/min for those in vertical configuration.

Moreover, a higher degree of disorder of deposited films with higher rates may explain a higher roughness. If we analyze the results obtained for ZnO, taking into account the deposition rate for evaporation and sputtering, we observed that this hypothesis is confirmed (see Table 4). However, the deposition rate could not be the only explanation in this case. The incidence angles and metal particles dynamics in a flow parallel or perpendicular to the substrate are not the same and certainly the metallic atoms dynamics near the substrate plays an important role on the growth process which influences subsequently the morphology of the oxide films. In the case of ZnO, we also remarked that doping with Al leads to a reduction of films roughness, no matter the deposition configuration.

The observations are in agreement with [11] for films deposited by sol-gel method.

Table4. Comparison of ZnO thin films roughness obtained by different methods in various configurations

Material/Configuration	Metal deposition method	Metal deposition rate (nm/s)	Oxide films roughness R_a (nm)	References
ZnO_horizontal	sputtering	1.2	116	this work
ZnO_horizontal	thermal vacuum evaporation	1.03	90	[18]
ZnO_vertical	thermal vacuum evaporation	0.6	40	[18]
ZnO_vertical	sputtering	0.3	28	this work

The morphology changes induced by the oxidation process of the metallic thin films, for both arrangements, were analyzed by scanning electron microscopy (SEM). For In:Sn metallic and oxide films, in horizontal configuration, we noticed a mixture of grains with different sizes and this morphology can explain the high values obtained for roughness. The surface is much more homogeneous for the films deposited in vertical configuration. The dimension of the grains is smaller and also the calculated values of the roughness were found smaller than for those samples deposited in horizontal arrangement.

For Zn and Zn:Al metallic films a homogeneous fine granular structure was observed. The oxidation process at 550°C resulted in the formation of ZnO nanowires on the film surface. This morphology is similar with that one observed by other authors [21,23] for ZnO films deposited on silicon (100) substrates. The length of these nanowires depends on the deposition geometry and the doping process and varies between 0.2 and 1.5 μm. The number of these “whiskers” is more important for the undoped films, in horizontal configuration.

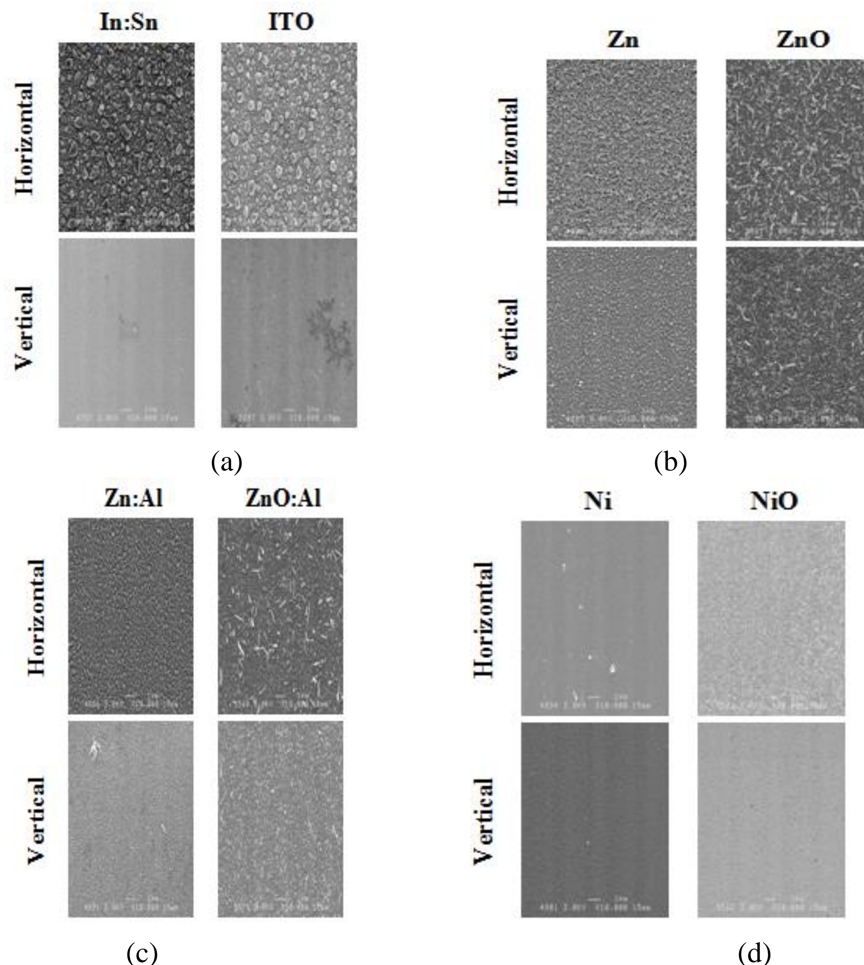

Fig. 3. SEM images for metallic and oxide thin films obtained in both arrangements, vertical and horizontal

3.3. Optical investigations

In Figs. 4a and 4b the transmission spectra for prepared oxide thin films in horizontal and vertical configurations are presented.

Due to their smaller thickness the films deposited in vertical arrangement had higher optical transmittance than those obtained in horizontal configuration. However, excepting ITO films, all the others have good transmission despite their thickness of about 4 times higher than that for the films deposited in vertical configuration. The low optical transmittance of the horizontal ITO films may be explained by the diffusion losses due to the high values of the roughness.

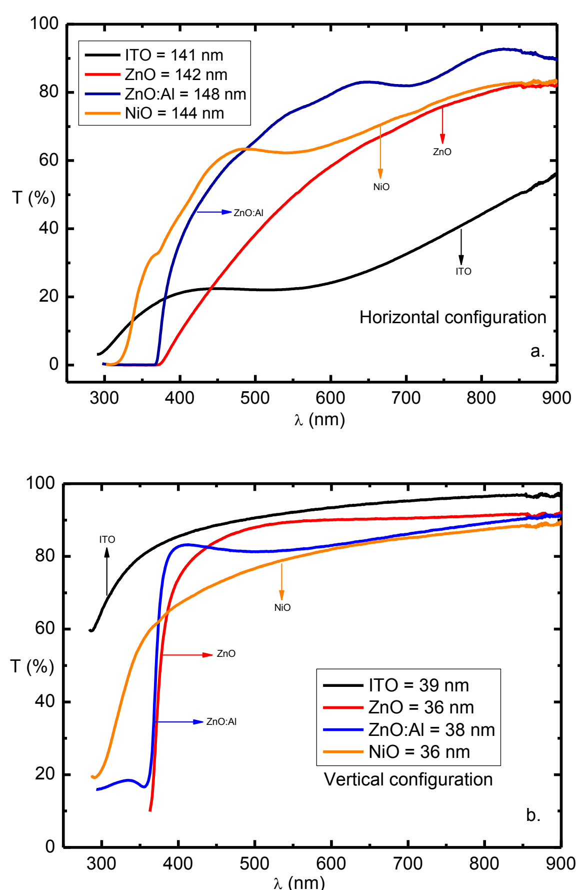

Fig. 4. Transmission spectra for ITO, ZnO, AZO and NiO prepared thin films

4. Conclusions

ITO, ZnO, Zn:Al and NiO thin films were obtained by thermal oxidation from metallic layers deposited onto optical glass substrates by magnetron sputtering, in two target-substrate configurations. All the oxide films have a well-defined crystalline structure without a pronounced preferentially growth direction. The size of the grains does not depend on the deposition geometry, while the roughness is highly influenced by the incidence angle of the sputtering flow to substrate. The morphology of the metallic layers influences that one of the oxide films. The prepared samples have a good transmittance in the visible range, higher than 80% for those obtained in vertical configuration. The present study confirms that direct thermal oxidation can be an alternative to obtain thin films that can be used in optoelectronic applications (as buffer layers, etc.).

Acknowledgements

Authors are grateful to the Region Pays de la Loire and Angers University for S.I. postdoc fellowship (No 2012-12029) and to Filmsolar ERA-NET-RUS European project for the financial support.

References

[1] M. Girtan, R. Mallet, Proceeding of the Romanian Academy Series a-Mathematics Physics Technical Sciences Information Science. **15**, 146 (2014).
[2] M. Girtan, Materials Science and Engineering B-Solid State Materials for Advanced Technology. **118**, 175 (2005).
[3] M. Girtan, A. Bouteville, G.G. Rusu, M. Rusu, J. Optoelectron. Adv. Mater. **8**, 27 (2006).
[4] C. Adominitei, D. Luca, M. Girtan, I. Sandu, V. Nica, A.V. Sandu, et al., J. Optoelectron. Adv. Mater. **15,** 519 (2013).
[5] I. Vaiciulis, M. Girtan, A. Stanculescu, L. Leontie, F. Habelhames, S. Antohe, Proceeding of the Romanian Academy Series a-Mathematics Physics Technical Sciences Information Science. **13**, 335 (2012).
[6] A.N. Banerjee, C.K. Ghosh, K.K. Chattopadhyay, H. Minoura, A.K. Sarkar, A. Akiba, et al., Thin Solid Films. **496**, 112 (2006).
[7] H. Zhang, C. Lei, H. Liu, C. Yuan, Applied Surface Science. **255**, 6054 (2009).
[8] M. Girtan, Solar Energy Materials and Solar Cells. **100**, 153 (2012).
[9] Y.M. Lu, W.S. Hwang, J.S. Yang, H.C. Chuang, Thin Solid Films. **420**, 54 (2002).
[10] M. Girtan, M. Socol, B. Pattier, M. Sylla, A. Stanculescu, Thin Solid Films. **519**, 573 (2010).
[11] F.Z. Ghomrani, S. Iftimie, N. Gabouze, A. Serier, M. Socol, A. Stanculescu, F. Sanchez, S. Antohe, M. Girtan, Optoelectron. Adv. Mater.-Rapid Commun. **5**, 247 (2011).
[12] A.V. Manole, M. Dobromir, M. Girtan, R. Mallet, G. Rusu, D. Luca, Ceramics International. **39**, 4771 (2013).
[13] D.Chapron, M. Girtan, J-Y Le Pommelec, A. Bouteville, J. Optoelectron. Adv. Mater. **9**, 902 (2007).
[14] M. Girtan, M. Kompitsas, R. Mallet, I. Fasaki, European Physical Journal-Applied Physics. 51 (2010) Article Number:33212
[15] M.Girtan, A. Vlad, R. Mallet, M.A. Bodea, J.D. Pedaring, A. Stanculescu, et al., Applied Surface Science. **274**, 306 (2013).
[16] M. Girtan, G.I. Rusu, G.G. Rusu, S. Gurlui, Applied Surface Science. **162,** 492 (2000).
[17] M. Girtan, G.I. Rusu, G.G. Rusu, Materials Science and Engineering B-Solid State Materials for Advanced Technology. **76**, 156 (2000).
[18] M. Girtan, G.G. Rusu, S. Dabos-Seignon, M. Rusu, Applied Surface Science. **254,** 4179 (2008).
[19] G.G. Rusu, M. Girtan, M. Rusu, Superlattices and Microstructures. **42**, 116 (2007).
[20] Y.D. Zhang, P.J. Li, B.J. Huang, Q.Y. Li, Z. Zheng, Optics Communications. **285,** 4290 (2012).
[21] L.C. Chao, S.Y. Tsai, C.N. Lin, C.C. Liau, and C.C. Ye, Materials Science in Semiconductor Processing. **16**, 1316 (2013) -1320.
[22] L.R. Covington, J.C. Moore, Thin Solid Films. **540**, 106 (2013).
[23] A. Zendehnam, M. Mirzaee, S. Miri, Applied Surface Science. **270**, 163 (2013).
[24] R.Q. Chen, C.W. Zou, X.D. Yan, W. Gao, Progress in Natural Science-Materials International. **21**, 81 (2011).
[25] M. Rusu, G.G. Rusu, M. Girtan, S.D. Seignon, Journal of Non-Crystalline Solids. **354**, 4461 (2008).

[26] Wolf, H, F, Semiconductors, 1971st ed., Wiley Interscience, New York.
[27] C. Besleaga, G. E.Stan, , A. C. Galca, L. Ion, S. Antohe, Applied Surface Science. **258**, 8819 (2012).
[28] V. A. Antohe, L. Gence, S. K. Srivastava, L. Piraux, Nanotechnology 23 (2012) Article Number: 255602
[29] C. Besleaga, L. Ion, V. Ghenescu, G. Socol, A. Radu, I. Arghir, C. Florica, S. Antohe, Thin Solid Films. **520,** 6803 (2012).
[30] S. Iftimie, C. Tazlaoanu, A. Radu, R. Constantineanu, C. Vancea, N. KorgancI, L. Ion, S. Antohe, Digest Journal of Nanomaterials and Biostructures. **9**, 213 (2014).
[31] C. Besleaga, L. Ion, S. Antohe, Romanian Reports in Physics, **66**, 993 (2014).
[32] C. Sima, L. Ion, C. Grigoriu, T. L. Mitran, S. Antohe, Digest Journal of Nanomaterials and Biostructures, **9**, 1479 (2014).
[33] V. A. Antohe, M. Mickan, F. Henry, R. Delamare, L. Gence, L. Piraux, Applied Surface Science, **313**, 607 (2014).